New Phytologist

# TNL-mediated immunity in *Arabidopsis* requires complex regulation of the redundant *ADR1* gene family

**Oliver Xiaoou Dong[1,2]*, Meixuezi Tong[1,2]*, Vera Bonardi[3], Farid El Kasmi[3], Virginia Woloshen[1,2], Lisa K. Wünsch[3], Jeffery L. Dangl[3,4] and Xin Li[1,2]**

[1]Michael Smith Laboratories, University of British Columbia, Vancouver, BC V6T 1Z4, Canada; [2]Department of Botany, University of British Columbia, Vancouver, BC V6T 1Z4, Canada; [3]Department of Biology, University of North Carolina, Chapel Hill, NC 27599-3280, USA; [4]Howard Hughes Medical Institute, University of North Carolina, Chapel Hill, NC 27599-3280, USA

Author for correspondence:
*Xin Li*
*Tel: +1 604 822 3155*
*Email: xinli@msl.ubc.ca*

Received: *9 July 2015*
Accepted: *24 November 2015*

*New Phytologist* (2016) **210:** 960–973
**doi**: 10.1111/nph.13821

**Key words:** ADR, ADR1, ADR1-L1, ADR1-L2, MUSE, nucleotide-binding leucine-rich repeat (NLR) receptor, plant immunity, SNC1.

## Summary

- Nucleotide-binding leucine-rich repeat proteins (NLRs) serve as intracellular immune receptors in animals and plants. Sensor NLRs perceive pathogen-derived effector molecules and trigger robust host defense. Recent studies revealed the role of three coiled-coil-type NLRs (CNLs) of the ADR1 family – ADR1, ADR1-L1 and ADR1-L2 – as redundant helper NLRs, whose function is required for defense mediated by multiple sensor NLRs.
- From a mutant *snc1*-enhancing (MUSE) forward genetic screen in *Arabidopsis* targeted to identify negative regulators of *snc1* that encodes a TIR-type NLR (TNL), we isolated two alleles of *muse15*, both carrying mutations in *ADR1-L1*. Interestingly, loss of *ADR1-L1* also enhances immunity-related phenotypes in other autoimmune mutants including *cpr1*, *bal* and *lsd1*. This immunity-enhancing effect is not mediated by increased SNC1 protein stability, nor is it fully dependent on the accumulation of the defense hormone salicylic acid (SA).
- Transcriptional analysis revealed an upregulation of *ADR1* and *ADR1-L2* in the *adr1-L1* background, which may overcompensate the loss of *ADR1-L1*, resulting in enhanced immunity. Interestingly, autoimmunity of *snc1* and *chs2*, which encode typical TNLs, is fully suppressed by the *adr1 triple* mutant, suggesting that the ADRs are required for TNL downstream signaling.
- This study extends our knowledge on the interplay among ADRs and reveals their complexity in defense regulation.

## Introduction

Defense responses against pathogens in plants are initiated mainly by two types of immune receptors (Chisholm *et al.*, 2006; Jones & Dangl, 2006). Plasma membrane-localized receptors perceive common pathogen associated molecular patters (PAMPs) and initiate downstream signal transduction events, leading to host responses including the production of reactive oxygen species, the deposition of callose and the increased expression of defense genes (Macho & Zipfel, 2014). Defense initiated through PAMP recognition is also known as PAMP-triggered immunity (PTI). By contrast, pathogen-encoded virulence factors (termed effector proteins) that have been delivered into host cells can be perceived by specific plant receptors typically belonging to the nucleotide-binding leucine-rich repeat protein (NLR; also known as Nod-like receptor) family. Activation of NLRs usually triggers more rapid and robust defense responses, and is often characterized by the occurrence of cell death at the site of infection termed the hypersensitive response (HR). Immunity triggered by NLR activation is also known as effector-triggered immunity (ETI). NLR proteins have important functions in plant immunity, yet the molecular mechanisms by which they are activated remain largely unclear.

Based on their N-termini, typical plant NLRs can be further classified into Toll-like/Interleukin 1 receptor (TIR)-type NLRs (TNLs) and coiled-coil NLRs (CNLs) (Dangl & Jones, 2001; Li *et al.*, 2015). In the mutant *suppressor of npr1-1, constitutive 1* (*snc1*), a gain-of-function mutation caused by a single amino acid substitution in TNL SNC1 leads to constitutive defense responses (Li *et al.*, 2001; Zhang *et al.*, 2003). Mutant *snc1* plants exhibit a characteristic autoimmune morphology including stunted growth and curled leaves (Li *et al.*, 2001). The severity of the *snc1* phenotypes correlates with the level of defense output, making *snc1* a useful tool for genetic screening. Indeed, from our previous *modifier of snc1* (*mos*) screen, 13 MOS proteins were identified that contribute to *SNC1*-mediated immunity (Johnson *et al.*, 2012).

In *Arabidopsis*, *ACTIVATED DISEASE RESISTANCE 1* (*ADR1, At1g33560*), *ADR1-LIKE 1* (*ADR1-L1, At4g33300*) and

*These authors contributed equally to this work.

*ADR1-LIKE 2* (*ADR1-L2*, *At5g04720*) all encode CNLs (Bonardi *et al.*, 2011). ADR1 family members function redundantly as positive regulators of basal defense and ETI mediated by the CNL protein RESISTANT TO PSEUDOMONAS SYRINGAE 2 (RPS2) and TNLs RECOGNITION OF PERONOSPERA PARASITICA 2 (RPP2) and RECOGNITION OF PERONOSPERA PARASITICA 4 (RPP4) (Bonardi *et al.*, 2011). A common feature of all three ADR1 family members is their N terminal coiled-coil domain, which resembles *Arabidopsis* RESISTANCE TO POWDERY MILDEW 8 (RPW8) and is referred to as $CC_R$ (Collier *et al.*, 2011). Another $CC_R$-NB-LRR protein is the N REQUIREMENT GENE 1 (NRG1) in *Nicotiana benthamiana*, which is required for the function of tobacco TNL N (Peart *et al.*, 2005; Collier *et al.*, 2011). These studies defined $CC_R$-NB-LRRs as helper NLRs in the signaling of other NLR proteins. It is important to note that their designation as helper NLRs does not discount a possible additional function as sensor NLRs in the context of as-yet-undiscovered effectors that could be recognized by this fascinating NLR class (Bonardi *et al.*, 2011).

In this study, we found that loss-of-function *adr1-L1* mutants enhance *snc1*. Quantitative RT-PCR analysis indicates that the enhanced autoimmunity may be due to transcriptional overcompensation by *ADR1* and *ADR1-L2* in the *adr1-L1* background. These results suggest that homeostasis of the ADR1 family is a key feature of their combined function as helper NLRs. In addition, *adr1 adr1-L1 adr1-L2* triple mutant (hereafter *adr1 triple*) completely suppresses the autoimmunity of *snc1* and *chs2-1* encoding typical TNLs, but not that of *slh1* and *uni-1D* encoding atypical TNL and CNL, respectively, indicating that the ADR1 helper NLR family serves as a critical signalling intermediate specifically for typical TNLs.

## Materials and Methods

### Plant materials used

*Arabidopsis thaliana* (L.) Heynh mutants used in this paper include *snc1* (Li *et al.*, 2001), *adr1-1* (Bonardi *et al.*, 2011), *adr1-L1-2* (Bonardi *et al.*, 2011), *adr1-L2-4* (Bonardi *et al.*, 2011), *bal* (Yi & Richards, 2009), *SNC1-GFP* and *snc1-GFP* (Xu *et al.*, 2014), *cpr1-3* (Cheng *et al.*, 2011), *lsd1-2* (Jabs *et al.*, 1996), *chs1-2* (Wang *et al.*, 2013), *chs2-1* (Huang *et al.*, 2010), *chs3-1* (Yang *et al.*, 2010), *pad4-1* (Glazebrook *et al.*, 1996), *eds5-3* (Nawrath & Metraux, 1999; Igari *et al.*, 2008), *uni-1D* (Igari *et al.*, 2008) and *slh1-9* (Noutoshi *et al.*, 2005).

### Growth conditions

For soil-grown plants, seeds were vernalized at 4°C for 2 d, sown onto sterile soil and transferred to plant growth rooms for either long day (22°C : 18°C, 16 h : 8 h, light : dark; *c.* 50% relative humidity) or short day (21°C : 18°C, 9 h : 15 h, light : dark; *c.* 50% relative humidity) or continuous light (22°C) conditions, as specified in figure legends. Phenotypes were scored at indicated time points. For all agar plate-grown seedlings, seeds were surface sterilized and sown on 0.5× MS agar plates, vernalized for 2 d and grown under long day conditions at 22°C.

### Plant genotyping

Mutant genotyping primers used are as follows: *adr1* (SAIL_842_B05) ADR1-1_s-Gen: CAA AGG ACG ATG ATG TTC GAG, ADR1-1_as: CGG ATT GTT CAC TAT AGT AAG G, LB_SAIL: TTT CAT AAC CAA TCT CGA TAC AC; *adr1-L1-1* (SAIL_302_C06) L1_1-s: ATG GCC ATC ACC GAT TTT TTC, adr1-L1_as: GTC AGG AAC AGG ATT TCC AG, LB_SAIL; *adr1-L2-4* (Salk_126422) PHX21_1_s: ATG GCA GAT ATA ATC GGC GG, PHX_ReT4_as: TGG GAG ATT GTG ACA CAG TC, LB1.3: ATT TTG CCG ATT TCG GAA C; *uni-1D* (Col-0, introgressed Ws line): VB14: GTT ATT TCT CGG AGA TAC CAT GC, VB15: GGA CAG TTT GAA ACA TCC ATG, Col-0 amplicon is *c.* 300 bp and *uni-1D* amplicon is *c.* 260 bp; *chs2* (*RPP4*) VB12: GAT TGA CCT TGT ATA TGA GGT GG, VB13: CAC TCA TCT TTG TCC CTT CCT TTT GAA, cut amplicon with *Mbo*II at 37°C o/n, Col-0 138 bp and 35 bp, *chs2* 138 bp and 60 bp; *chs3* VB10: TCC TCC TTA CTC CTT GTG AGA C, VB11: TCT CTC TCT CAC TCT CTT CGT AGT TCC CA, cut amplicon with *Bci*130I at 37°C or 8 h, Col-0 170 bp and 25 bp, *chs3* 194 bp; *slh1-9* LW1: GTT ATA TCG ACG TTG GAT GCA G, LW2: CCA GCA AGT TTA GGA TGA TTA CG, cut amplicon with *Dde*I at 37°C o/n, Col-0 260 bp and 120 bp, *slh1-9* 380 bp. *cpr1* (SALK_045148) LP: TTT CGT AAA TTT TTA CAC AAA ATC G, RP: TGT GAG TAG CCT TGT CTT GGG. To genotype homozygous *eds5-3*, SNP primers F: ACT TCA GAG CGG TGA TCA GA and R: CAT CAA CGG TCC ACA AGT C were used. All mutant combinations were confirmed by genotyping.

### Map-based cloning of *muse15*

Rough and fine mapping of *muse15* was performed as previously described (Huang *et al.*, 2013). Primers involved in mapping were designed based on Monsanto *Arabidopsis* polymorphism and Landsberg sequence collections (Jander *et al.*, 2002). Marker primers used include: FCA8 F: CTC CAA GCT TAG TGC AAC TC, R: TGA ACT GCA TTA ACA TGG AAC; T13J8 F: ATG TTC CCA GGC TCC TTC CA, R: GAG ATG TGG GAC AAG TGA CC; F8D20 F: TTG ATC TGA ATA GGT CCC CC, R: ACT GTT GCG ATA ATG CAG TG; F26P21 F: TCT TCA ATG ATA CCC ATC CC, R: ATA TTT GCG ATT TCT ATT TTG GAG; F17I5 F: ATG GGC TAG ATA ATT TCT AAG G, R: AAT GAA TTG TTA CAT GAG GTC G.

### Infection assay

Ten-day-old soil-grown *Arabidopsis* seedlings were spray-inoculated with freshly harvested *Hyaloperonospora arabidopsidis* (*H.a.*) Noco2 spores re-suspended in water. Infected plants were kept at 18°C with 80% humidity for 7 d before data collection. Growth of the pathogen was measured by totaling the number of spores per gram of fresh weight (FW).

### Total salicylic acid (SA) measurement

Leaf tissue was harvested from 4-wk-old *Arabidopsis* plants and homogenized and mixed with 0.2 ml 90% methanol. Samples were sonicated using a water bath sonicator for 20 min and centrifuged at 15 000 ***g*** for 20 min. 0.3 ml 100% methanol was added to the debris for a second extraction. Samples were thoroughly vortexed, spun down again and the supernatant from the two extractions were combined and left to dry overnight at room temperature. On the next day, 0.1 ml β-glucosidase solution (80 unit $ml^{-1}$ β-glucosidase (Sigma G0395), in 0.1 M NaAc, pH 5.2) was added to each sample. Samples were vortexed and sonicated for 5 min and incubated at 37°C for 90 min. 0.5 ml 0.5% TCA (Sigma T6399) was added to the samples. Samples were spun down at 15 000 ***g*** for 15 min and the supernatant was transferred to a new set of tubes and extracted three times using extraction medium (ethylacetate : cyclopentant : isopropanol = 100 : 99 : 1). The combined extraction product was left to dry overnight at room temperature. SA samples were dissolved in mobile phase (0.2 M KAc, 0.5 mM EDTA, pH 5.0) and the quantity of SA was measured using HPLC. The abundance of SA was presented as μg SA per gram FW of plant tissue.

### RNA extraction and gene expression analyses

Total RNA was extracted from 2-wk-old seedlings grown on 0.5× MS medium or 4-wk-old soil grown plants using Totally RNA Kit (Ambion). Reverse transcription was performed using Easyscript Reverse Transcription Kit (ABM, Richmond, BC, Canada). Semi-quantitative PCR was performed as described before (Zhang *et al.*, 2003). Real-time PCR was performed using a Perfect Realtime Kit (Takara, Beijing, China). Sequences of the primers used are *ACT1* F: CGA TGA AGC TCA ATC CAA ACG A, R: CAG AGT CGA GCA CAA TAC CG; *ACT7* F: GGT GTC ATG GTT GGT ATG GGT C, R: CCT CTG TGA GTA GAA CTG GGT GC; *PR1* F: GTA GGT GCT CTT GTT CTT CCC, R: CAC ATA ATT CCC ACG AGG ATC; *PR2* F: GCT TCC TTC TTC AAC CAC ACA GC, R: CGT TGA TGT ACC GGA ATC TGA C; *SNC1* F: CTG GGA TAA GTT GTA TCG TGT TG, R: AGA TGT CCC CGA TGT CAT CCG; *ADR1* F: ATA GTG AAC AAT CCG AGG TT, R: TTT CAT CCA TTT CCC CTG T; *ADR1-L2* F: CTT GTG AAA GAT CCA AGG TT, R: TGA GTC ATT TCT CCT GTG T.

### Ion leakage measurement

Rosette leaves were harvested from 4-wk-old plants and six leaf discs (6 mm diameter) were collected and then floated in 20 ml water for 30 min. These leaf discs were transferred to tubes containing 6 ml distilled water. Conductivity of the solution (μSiemens $cm^{-1}$) was determined with a conductivity meter (Model 2052; Amber Science, San Diego, CA, USA) at the indicated time points. For mutants that exhibit cell death at earlier developmental stages, the experiment was performed with two whole 2-wk-old seedlings.

### Protein extraction and western blot analysis

Total protein was extracted from 2-wk-old *Arabidopsis* seedlings grown on 0.5× MS medium. The whole extraction was performed either on ice or in a 4°C cold room. Tissues were homogenized and mixed with extraction buffer (100 mM Tris–HCl pH 8.0, 0.1% SDS and 2% β-mercaptoethanol). Samples were vortexed and centrifuged at 15 000 ***g*** for 10 min. SDS loading buffer was added to supernatants and samples were boiled for 5 min before loading onto a SDS-PAGE gel. After electrophoresis, separated protein samples were transferred to a membrane and subjected to western blot analyses. The anti-SNC1 antibody was generated against a SNC1-specific peptide from rabbit (Li *et al.*, 2010). Protein bands were quantified using ImageJ (http://imagej.nih.gov).

## Results

### Isolation and characterization of two allelic *muse* mutants from a modified *snc1* enhancer screen

We screened for novel negative regulators of plant immunity in either *snc1 mos4* or *snc1 mos2 npr1* genetic backgrounds using ethyl methanesulfonate (EMS) as mutagen (Huang *et al.*, 2013). Two *muse* mutants, *muse15-1* and *muse15-2,* were isolated independently from the *snc1 mos4* and *snc1 mos2 npr1* genetic backgrounds, respectively (Fig. 1a,b). Both mutants altered the *snc1 mos* morphology back to *snc1*-like. Segregation from backcrossed $F_2$ populations suggested the presence of a single recessive mutation in each mutant. *snc1 mos4 muse15-1* and *snc1 mos2 npr1 muse15-2* failed to complement each other in an $F_1$ allelism test (Fig. 1c), suggesting that they carry mutations in the same gene. Besides their dwarf stature and curled leaves (Fig. 1a,b), both mutants exhibited increased expression of defense marker genes *PR1* and *PR2* (Fig. 1d), and enhanced disease resistance to the virulent oomycete pathogen *H.a.* Noco2 (Fig. 1e). As both *muse15* alleles are recessive, they likely carry loss-of-function mutations that enhance the *snc1* autoimmune phenotypes.

### *MUSE15* encodes ADR1-L1, a $CC_R$-NB-LRR protein

In order to map the *muse15-1* and *muse15-2* mutations, the original enhancer mutants (in Col-0 ecotype) were crossed with Landsberg *erecta* (L*er*). The $F_1$ individuals were selfed to generate a mapping population. Among $F_2$s, individuals displaying enhanced *snc1* phenotypes were selected for linkage analysis. Consistent with the allelism test result (Fig. 1c), crude mapping revealed that *muse15-1* and *muse15-2* are both located at the bottom of chromosome 4. Subsequently, *muse15-1* was further mapped between markers F26P21 and F17I5 (Fig. 2a). To identify the molecular lesion in *muse15-2*, nuclear DNA from plants homozygous for *muse15-2* was used for whole-genome resequencing by an Illumina sequencer. When the *muse15-2* sequence was compared with wild-type (WT) Col-0 reference sequence in the region between F26P21 and F17I5, a single G to A mutation was identified, which is consistent with EMS

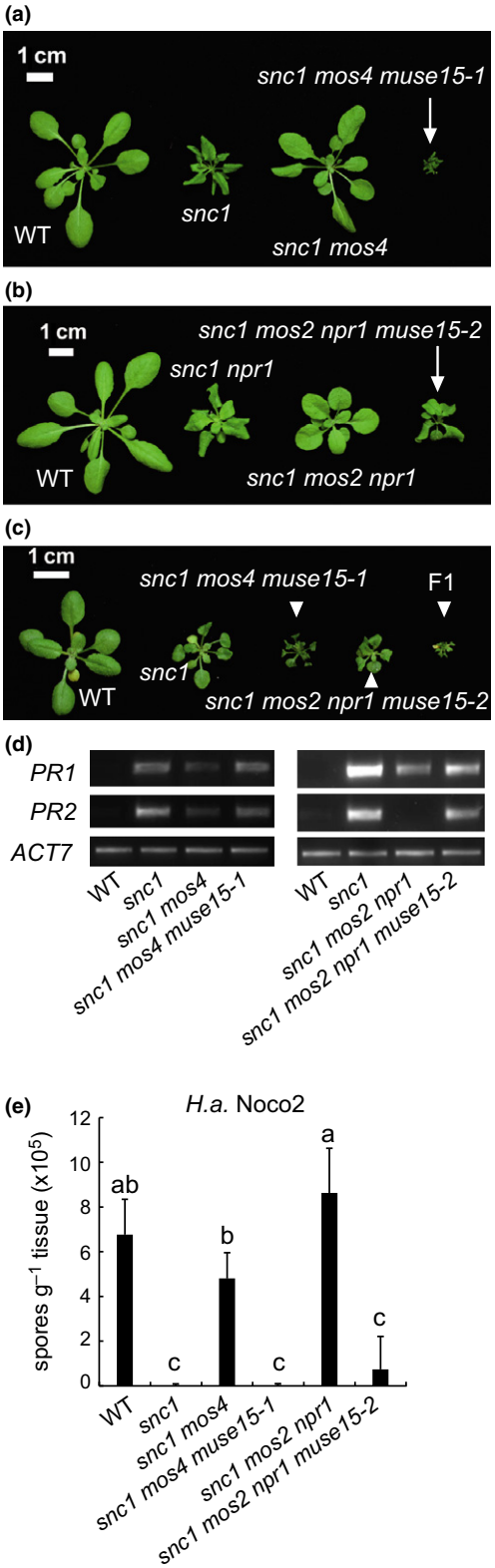


**Fig. 1** Two allelic *muse15* mutants enhance immunity in the *snc1 mos4* or *snc1 mos2 npr1* background. (a) Morphological phenotypes of 4-wk-old Col-0 wild-type (WT), *snc1*, *snc1 mos4* and *snc1 mos4 muse15-1* plants grown at 22°C under long day conditions (16 h : 8 h, light : dark). (b) Morphological phenotypes of 4-wk-old WT, *snc1*, *snc1 mos2 npr1* and *snc1 mos2 npr1 muse15-2* plants grown at 22°C under long day conditions. (c) Morphological phenotypes of 3-wk-old WT, *snc1*, *snc1 mos4 muse15-1*, *snc1 mos2 npr1 muse15-2* and an $F_1$ plant from the cross between *snc1 mos4 muse15-1* and *snc1 mos2 npr1 muse15-2* grown at 22°C under long day conditions. (d) Expression of defense marker genes *PR1* and *PR2* in WT, *snc1*, *snc1 mos4*, *snc1 mos4 muse15-1*, *snc1 mos2 npr1* and *snc1 mos2 npr1 muse15-2* plants. Reverse transcription (RT)-PCR was performed on 2-wk-old seedlings grown on 0.5× MS plates. *ACT7* was included as loading control. (e) Growth of *Hyaloperonospora arabidopsidis* (*H.a.*) Noco2 7 d after spray-infection with $10^5$ spores $ml^{-1}$ inoculum on WT, *snc1*, *snc1 mos4*, *snc1 mos4 muse15-1*, *snc1 mos2 npr1* and *snc1 mos2 npr1 muse15-2* plants. One-way ANOVA was used to calculate the statistical significance between genotypes, as indicated by different letters ($P < 0.01$). Bars represent mean ± SD ($n = 4$).

mutagenesis. This mutation is predicted to cause a single amino acid Pro513 to Leu change in the polypeptide encoded by *ADR1-L1* (*At4g33300*) (Fig. 2b). We then sequenced *ADR1-L1* in homozygous *muse15-1* plants by the Sanger method and identified a separate G to A mutation located at an exon–intron junction (Fig. 2c). This mutation presumably alters the splicing pattern of the gene, leading to early truncation of the encoded protein.

In order to further confirm that the two mutations we identified in *muse15* alleles are responsible for the *snc1*-enhancing phenotypes, we crossed *snc1* with a known loss-of-function T-DNA *adr1-L1* allele, SAIL_302_C06 (Bonardi *et al.*, 2011). Compared with *snc1* plants, the *snc1 adr1-L1* double mutant exhibits more severe stunted growth and curled leaves, which is consistent with the *snc1*-enhancing phenotypes of *muse15-1* and *muse15-2* mutants (Fig. 2d,e). Taken together, we conclude that *MUSE15* is *ADR1-L1* and that the new, herein identified *adr1-L1* alleles are also loss-of-function mutants.

*ADR1-L1* encodes an RPW8 $CC_R$-type CNL protein (Fig. 2b). Together with ADR1 and ADR1-L2, these three NLRs function redundantly to regulate the accumulation of the defense hormone SA (Bonardi *et al.*, 2011). *adr1 triple* mutant exhibit enhanced susceptibility to virulent and avirulent pathogens, suggesting that ADR1 proteins function redundantly in immune signaling (Bonardi *et al.*, 2011). However, the *snc1*-enhancing phenotypes of *adr1-L1* observed here are seemingly opposite to the *adr1 triple* mutant phenotypes, suggesting that ADR1-L1 has a unique negative regulatory role in defense besides its redundant positive functions with ADR1 and ADR1-L2.

## ADR1-L1 does not affect SNC1 protein turnover

Several previously described *muse* mutants exhibit increased SNC1 protein accumulation (Huang *et al.*, 2014a,b; Xu *et al.*, 2015), and therefore these MUSE proteins contribute to SNC1 turnover. To address why *adr1-L1* enhances *snc1*, we first tested whether ADR1-L1 regulates the autoimmune phenotypes in *snc1* through affecting SNC1 protein accumulation. SNC1 protein level is increased significantly in *snc1 adr1-L1* compared to that in *snc1* (Fig. 3a). However, this accumulation correlates with the

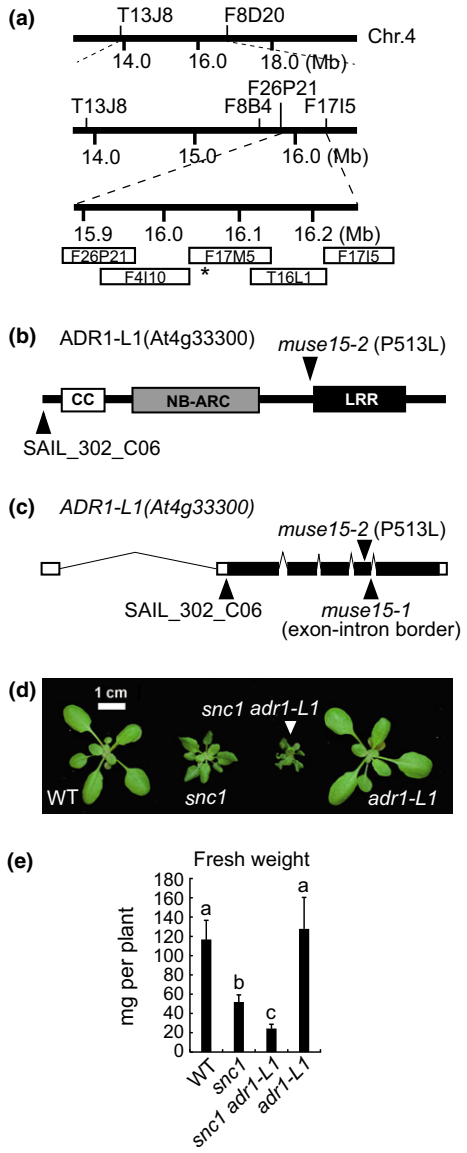


**Fig. 2** Positional cloning of *muse15* in *Arabidopsis*. (a) Map position of *muse15*. The asterisk indicates the site of *muse15-2* mutation. (b) Schematic diagram showing the predicted ADR1-L1 protein structure with arrows indicating the sites of mutations in *muse15-2* and *adr1-L1* (SAIL_302_C06). (c) Schematic diagram showing the predicted *ADR1-L1* gene structure with arrows indicating the sites of mutations in *muse15-1*, *muse15-2* and SAIL_302_C06. (d) Morphological phenotypes of 4-wk-old WT, *snc1*, *snc1 adr1-L1* and *adr1-L1* plants grown at 22°C under long day conditions. (e) Fresh weights of 4-wk-old WT, *snc1*, *snc1 adr1-L1* and *adr1-L1* plants grown at 22°C under long day conditions. One-way ANOVA was used to calculate the statistical significance between genotypes, as indicated by different letters ($P < 0.01$). Bars represent mean ± SD ($n = 20$).

enhanced *SNC1* transcription observed in the double mutant (Fig. 3b). To avoid the feedback upregulation of *SNC1* transcription as in *snc1 adr1-L1*, we examined SNC1 protein accumulation in *adr1-L1*. No difference in steady-state SNC1 levels was observed between WT and *adr1-L1* (Fig. 3c). Similarly, in the WT-like *snc1 pad4-1 adr1-L1* triple mutant, where the SA-dependent positive feedback transcriptional upregulation of *SNC1* is blocked, no significant difference in SNC1 protein level was observed when compared to *snc1 pad4-1* (Fig. 3d,e). These results suggest that ADR1-L1 does not enhance the autoimmune phenotypes in *snc1* through affecting SNC1 protein turnover.

## The autoimmune-enhancing phenotype of *snc1 adr1-L1* is not fully dependent on SA accumulation

SA plays a major role in defense amplification. Because the autoimmune phenotypes of *snc1* are partly dependent on SA levels (Zhang *et al.*, 2003), and the ADR1 family regulates SA accumulation (Bonardi *et al.*, 2011), we tested whether the *snc1*-enhancing phenotypes in *snc1 adr1-L1* depend on SA accumulation. The SA deficient mutant *enhanced disease susceptibility 5* (*eds5*) was crossed with *snc1 adr1-L1* to generate the *snc1 eds5-3 adr1-L1* triple mutant. Although the triple mutant partially rescued the *snc1 adr1-L1* phenotype, it was significantly smaller than *snc1 eds5-3* (Fig. 4a,b), suggesting that the *snc1*-enhancing effects observed from *adr1-L1* are not fully dependent on SA accumulation.

## Loss of ADR1-L1 leads to transcriptional upregulation of *ADR1* and *ADR1-L2*

Constitutive increase in steady-state NLR protein levels often results in autoimmune phenotypes (Tang *et al.*, 1999; Tao *et al.*, 2000; Frost *et al.*, 2004; Cheng *et al.*, 2011; Gou *et al.*, 2012). Not surprisingly, overexpression of *ADR1* also leads to autoimmunity (Grant *et al.*, 2003). We therefore tested if the loss of *ADR1-L1* could be overcompensated by increased expression of its paralogs, *ADR1* and *ADR1-L2*. When we compared the transcript levels of *ADR1* and *ADR1-L2* in WT, *adr1-L1*, *snc1* and *snc1 adr1-L1*, we noted a consistent two-fold increase in *ADR1* transcript levels, and a 50% increase in *ADR1-L2* expression in *snc1 adr1-L1* compared to *snc1* (Fig. 5a,b). We also consistently observed a slight, yet not always significant, increase of both *ADR1* and *ADR1-L2* transcripts in *adr1-L1* compared to WT (Fig. 5a,b; Supporting Information Fig. S1). *ADR1* seems to compensate more than *ADR1-L2*.

## *adr1-L1* enhances the autoimmune phenotypes in some, but not all autoimmune mutants

In order to test the specificity of the immunity-enhancing effects of *adr1-L1*, we crossed the T-DNA knockout allele of *adr1-L1* with a collection of autoimmune mutants. Increased SNC1 protein level leads to a similar autoimmune phenotype as that observed in mutant *snc1* (Xu *et al.*, 2014). Therefore, we crossed *adr1-L1* with a set of genetic backgrounds that exhibit increased SNC1 protein levels. These included *constitutive expressor of PR genes 1* (*cpr1*), *bal* and *SNC1* transgenic overexpression lines. *CPR1* encodes an F-box protein that facilitates the degradation of SNC1 and RPS2 (Cheng *et al.*, 2011). In knockout mutant *cpr1-3*, over-accumulation of SNC1 contributes partly to its autoimmune phenotypes (Cheng *et al.*, 2011). In the *cpr1-3 adr1-L1* double mutant, the autoimmune phenotypes of *cpr1-3* were

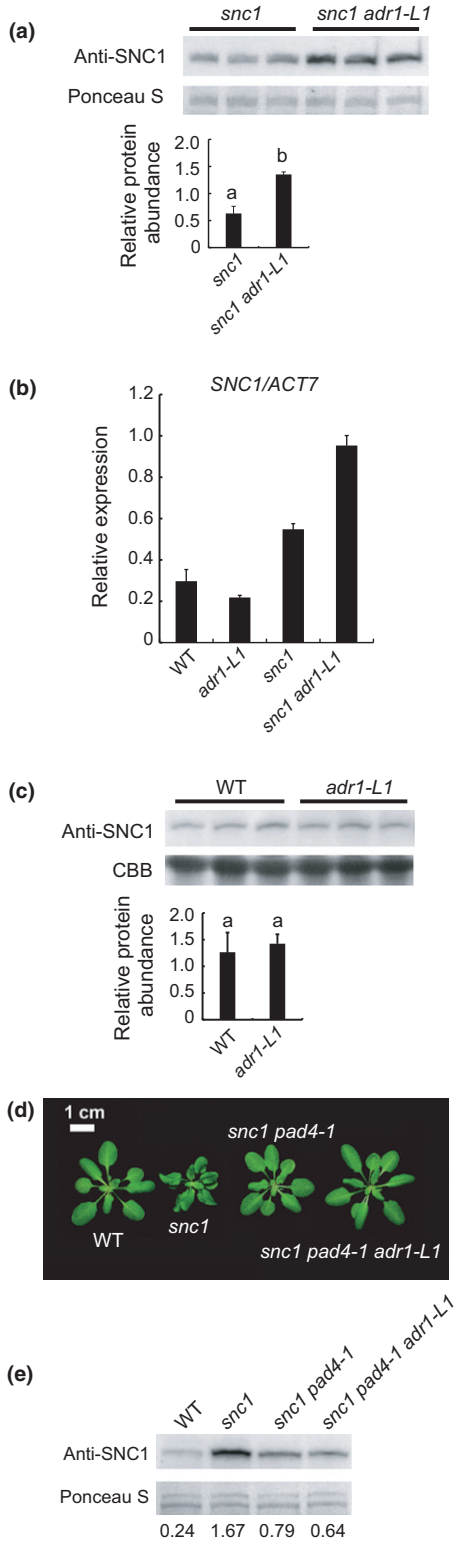


**Fig. 3** ADR1-L1 does not affect SNC1 turnover in *Arabidopsis*. (a) Upper: Western blot analysis using an anti-SNC1 antibody. Leaf total protein was extracted from 4-wk-old plants grown at 22°C under long day conditions. Lower: quantification of the relative intensity of the SNC1 bands to nonspecific bands in Ponceau S staining in the upper panel. A pairwise *t*-test was used to calculate the statistical significance between genotypes, as indicated by different letters ($P < 0.05$). Bars represent mean ± SD ($n = 3$). (b) *SNC1* transcript levels in WT, *adr1-L1*, *snc1* and *snc1 adr1-L1* plants. qRT-PCR was performed on 4-wk-old plants grown at 22°C under long day conditions. *ACT7* was used to normalize the transcript levels. Arbitrary units were used to show the relative abundance of *SNC1* transcript levels as compared to that in WT. Bars represent mean ± SD ($n = 3$). (c) Upper: Western blot analysis using an anti-SNC1 antibody. Leaf total protein was extracted from 4-wk-old plants grown at 22°C under long day conditions. Lower: quantification of the relative intensity of the SNC1 bands to nonspecific bands from Coomassie Brilliant Blue (CBB) staining in the upper panel. Pairwise *t*-test was used to calculate the statistical significance between genotypes, as indicated by different letters ($P < 0.01$). Bars represent mean ± SD ($n = 3$). (d) Morphological phenotypes of 4-wk-old WT, *snc1*, *snc1 pad4-1* and *snc1 pad4-1 adr1-L1* plants grown at 22°C under long day conditions. (e) Western blot analysis using an anti-SNC1 antibody on the indicated genotypes. Leaf total protein was extracted from 4-wk-old plants grown at 22°C under long day conditions. Numbers underneath indicate the relative intensity of the SNC1 band to a nonspecific band in Ponceau S staining.

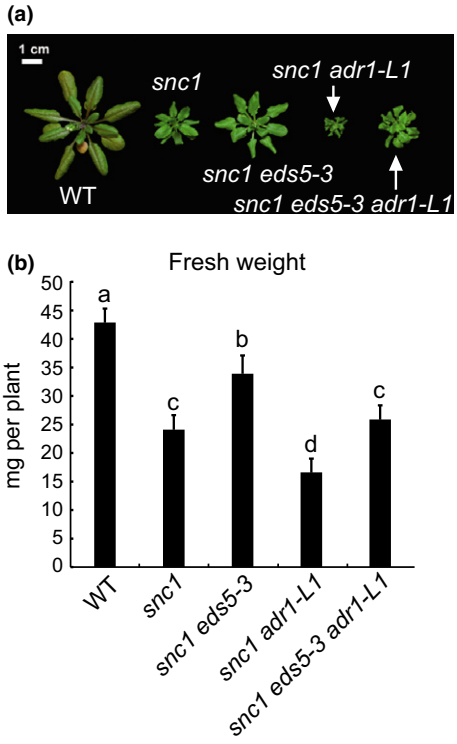


**Fig. 4** The defense-enhancing phenotypes in *snc1 adr1-L1* are not fully dependent on salicylic acid (SA) accumulation in *Arabidopsis*. (a) Morphological phenotypes of 4-wk-old WT, *snc1*, *snc1 eds5-3*, *snc1 adr1-L1* and *snc1 eds5-3 adr1-L1* plants grown at 22°C under long day conditions. (b) Fresh weights of 3-wk-old WT, *snc1*, *snc1 eds5-3*, *snc1 adr1-L1* and *snc1 eds5-3 adr1-L1* plants grown at 22°C under long day conditions. One-way ANOVA was used to calculate the statistical significance between genotypes, as indicated by different letters ($P < 0.001$). Bars represent mean ± SD ($n = 10$).

significantly enhanced by *adr1-L1*, as illustrated by plant size (Fig. 5c), fresh weight (Fig. 5d) and total SA measurements of the mutant plants (Fig. 5e). A duplication within the *RPP4* cluster also results in heightened expression of *SNC1* in the *bal* mutant, resulting in *snc1*-like autoimmunity (Stokes *et al.*, 2002; Yi &

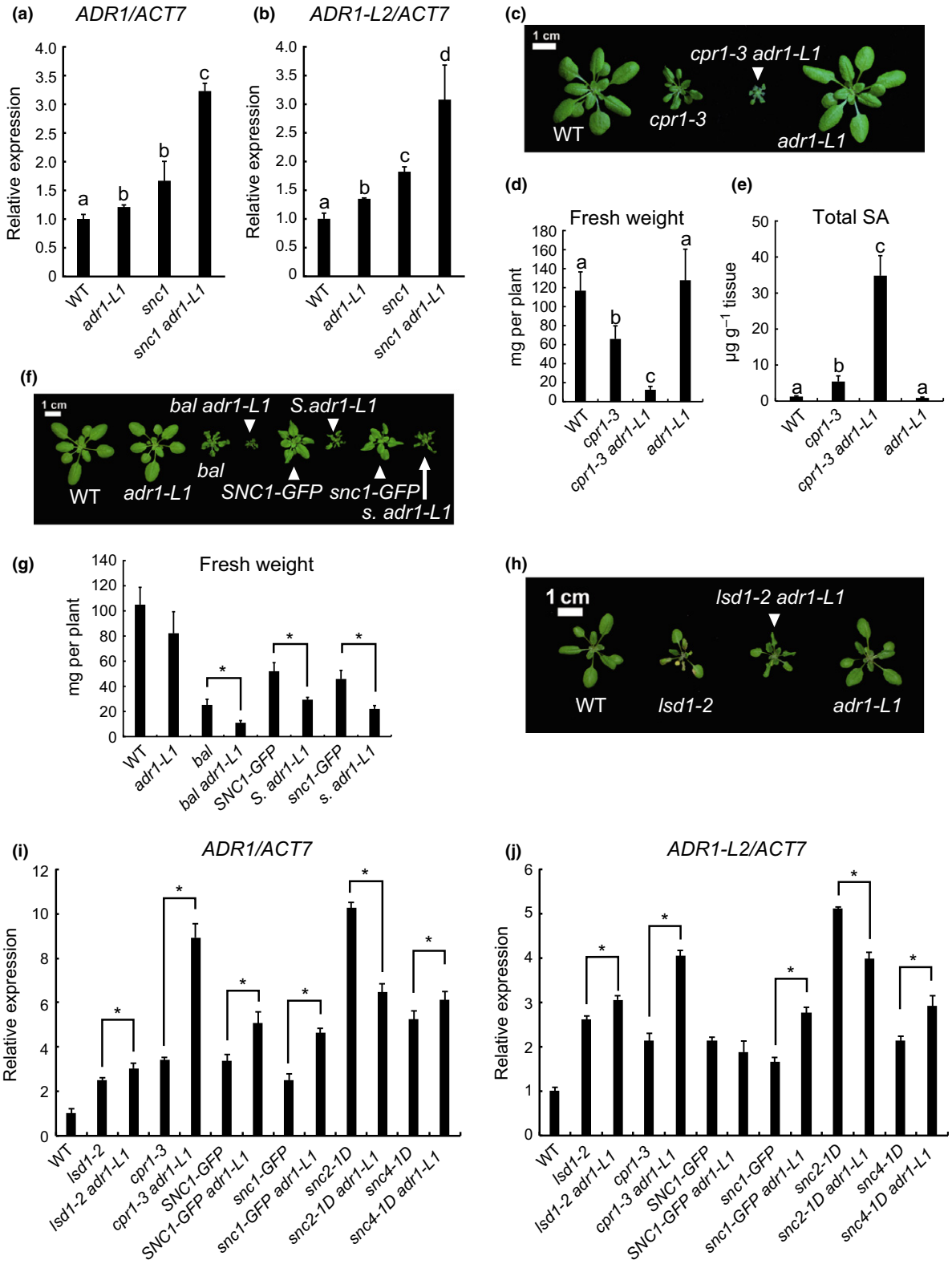


Richards, 2009). Similarly, transgenic overexpression of WT *SNC1* or mutant *snc1* in Col-0 results in severe autoimmune phenotypes (Xu *et al.*, 2014). The autoimmune phenotypes of *bal* and transgenic *SNC1*- or *snc1*-overexpression lines were all enhanced by *adr1-L1* (Fig. 5f,g), suggesting that SNC1-mediated defense can be enhanced by knocking out *ADR1-L1*, independent of the gain-of-function mutation in *snc1*. Such enhancement does not rely on the chromosomal location of the *SNC1* gene, as manifested by the phenotypic enhancement of transgenic *SNC1*- or *snc1*-overexpression lines by *adr1-L1*.

**Fig. 5** *adr1-L1* enhances the autoimmune phenotypes of some, but not all, autoimmune mutants tested, leading to increased *ADR1* and *ADR1-L2* transcript levels in *Arabidopsis*. (a, b) *ADR1* and *ADR1-L2* transcript levels in the indicated genotypes. qRT-PCR was performed on 2-wk-old seedlings grown on 0.5× MS plates. *ACT7* was used to normalize the transcript levels. Values for WT were set as 1.0. Pairwise *t*-tests were used to calculate the statistical significance between genotypes, as indicated by different letters ($P < 0.05$). Bars represent mean ± SD ($n = 3$). The whole experiment involving all four genotypes was biologically repeated twice. Experiment with WT and *adr1-L1* was biologically repeated for two additional times (four times in total). Refer to Supporting Information Fig. S1 for data from the other three biological repeats on WT and *adr1-L1*. (c) Morphological phenotypes of 4-wk-old WT, *cpr1-3*, *cpr1-3 adr1-L1* and *adr1-L1* plants grown at 22°C under long day conditions. (d) Fresh weights of 4-wk-old WT, *cpr1-3*, *cpr1-3 adr1-L1* and *adr1-L1* plants grown at 22°C under long day conditions. One-way ANOVA was used to calculate the statistical significance between genotypes, as indicated by different letters ($P < 0.01$). Bars represent mean ± SD ($n = 20$). (e) Total salicylic acid (SA) levels of 4-wk-old WT, *cpr1-3*, *cpr1-3 adr1-L1* and *adr1-L1* plants grown at 22°C under long day conditions. Multiple *t*-tests were used to calculate the statistical significance between genotypes, as indicated by different letters ($P < 0.01$). Bars represent mean ± SD ($n = 4$). (f) Morphological phenotypes of 4-wk-old WT, *adr1-L1*, *bal*, *bal adr1-L1*, *SNC1-GFP*, *SNC1-GFP adr1-L1* (*S. adr1-L1*), *snc1-GFP* and *snc1-GFP adr1-L1* (*s. adr1-L1*) plants grown at 22°C under long day conditions. (g) Fresh weights of 4-wk-old WT, *adr1-L1*, *bal*, *bal adr1-L1*, *SNC1-GFP*, *SNC1-GFP* in *adr1-L1*, *snc1-GFP* and *snc1-GFP* in *adr1-L1* plants grown at 22°C under long day conditions. Pairwise *t*-tests were used to calculate the statistical significance between genotypes, as indicated by asterisks ($P < 0.001$). Bars represent mean ± SD ($n = 5$). (h) Morphological phenotypes of 3-wk-old WT, *lsd1-2*, *lsd1-2 adr1-L1* and *adr1-L1* plants grown at 22°C under long day conditions. (i, j) *ADR1* and *ADR1-L2* transcript levels in the indicated genotypes. qRT-PCR was performed on 3-wk-old soil-grown plants grown at 22°C under long day conditions. *ACT7* was used to normalize the transcript levels. Values for WT were set as 1.0. Pairwise *t*-tests were used to calculate the statistical significance between genotypes, as indicated by asterisks ($P < 0.05$). Bars represent mean ± SD ($n = 3$). The whole experiment was biologically repeated twice with similar trends.

*Lesion Simulating Disease 1* (*LSD1*) encodes a zinc finger protein involved in the negative regulation of pathogen-induced cell death (Dietrich *et al.*, 1997). Loss-of-function mutant *lsd1-2* plants exhibit abnormal superoxide accumulation and excessive cell death upon induction (Jabs *et al.*, 1996). Under our growth condition, the *lsd1-2 adr1-L1* double mutant exhibited a *snc1*-like autoimmune phenotype (Fig. 5h), which was absent in the *lsd1-2* single mutant. The *lsd1-2* mutant exhibited spontaneous cell death (Fig. 5h), which differs from the previously reported inducible cell death phenotype of *lsd1-2* (Jabs *et al.*, 1996). This could be due to the difference in the light regime used for plant growth. Interestingly, the cell death phenotype of *lsd1-2* is suppressed by *adr1-L1* (Fig. S2a). Overall, the *lsd1 adr1-L1* phenotypes suggest that the immunity-enhancing effect of *adr1-L1* is also active in the *lsd1-2* background, and is not specific to *snc1*.

In the autoimmune mutant *suppressor of npr1-1, constitutive 2* (*snc2-1D*), a gain-of-function mutation in a receptor-like protein (RLP) confers constitutively activated defense responses (Zhang *et al.*, 2010). SNC2 likely functions with other membrane-bound proteins in the perception of unidentified PAMPs (Yang *et al.*, 2012). As shown in Fig. S3(a), the autoimmune phenotype of *snc2-1D* was not enhanced by *adr1-L1*. Similarly, the autoimmune phenotypes of *snc4-1D*, which carries a gain-of-function mutation in the receptor-like kinase (RLK) SUPPRESSOR OF NPR1-1, CONSTITUTIVE 4 (SNC4) that leads to constitutive defense responses (Bi *et al.*, 2010), were not enhanced by *adr1-L1* either (Fig. S3b). These results suggest that *adr1-L1* does not enhance autoimmunity triggered by gain-of-function mutants of these specific RLP and RLK.

In the mutant *chilling sensitive 1* (*chs1-2*), a missense mutation in a TIR-NB protein causes autoimmune phenotypes under chilling conditions (Wang *et al.*, 2013). Under our growth condition, *chs1-2* exhibited dwarfed stature and curled leaves, yet these phenotypes were not enhanced in *chs1-2 adr1-L1* (Fig. S3c). The difference in the *chs1-2* phenotypes that we observed under 22°C and those previously reported (Wang *et al.*, 2013) are likely due to differences in growth condition. Another chilling sensitive mutant *chilling sensitive 2* (*chs2-1*) harbors a gain-of-function mutation in *RPP4*, which encodes a typical TNL (Huang *et al.*, 2010). The autoimmune phenotypes of *chs2-1* were not enhanced by *adr1-L1* either (Fig. S3d). In the mutant *chilling sensitive 3* (*chs3-1*), a mutation in the C-terminal LIM domain of the atypical TNL protein CHS3 leads to chilling sensitivity and constitutive activated defense responses, which can be alleviated at higher temperatures (Yang *et al.*, 2010). We did not detect enhancement of *chs3-1* by *adr1-L1* (Fig. S3e). Additionally, the cell death phenotype under chilling condition in *chs3-1*, but not in *chs1-2*, was suppressed by *adr1-L1* (Fig. S2b). These results suggest that loss of ADR1-L1 function does not affect the defense responses mediated through CHS1, CHS2 or CHS3. Taken together, the autoimmunity-enhancing ability of *adr1-L1* seems to be specific to only certain autoimmune mutant backgrounds.

In order to further test whether the upregulation of *ADR1* and *ADR1-L2* transcription overcompensates for the loss of ADR1-L1, we compared the transcript levels of *ADR1* and *ADR1-L2* in additional autoimmune mutants with or without *adr1-L1* mutation (Fig. 5i,j). We observed significantly increased *ADR1* transcription with *adr1-L1* under all mutant backgrounds tested except for *snc2-1D*, and significantly increased *ADR1-L2* transcription in *adr1-L1* under all mutant backgrounds tested except for the *SNC1*-overexpressing line (difference insignificant) and *snc2-1D* (Fig. 5i, j). Therefore, the upregulation of *ADR1* and *ADR1-L2* transcription is not only specific to the *snc1* mutant background.

Taken together, these results suggest that *ADR1* and *ADR1-L2* transcriptions are both upregulated in mutant *adr1-L1*, which may compensate for the loss of *ADR1-L1*. This overcompensation becomes more obvious in autoimmune backgrounds.

## Genetic interplay among the three redundant *ADR1* gene family members

In order to further address whether the immunity-enhancing effects of *adr1-L1* are dependent on ADR1 and ADR1-L2, we introduced knockout mutations in *adr1* and *adr1-L2* into the *snc1*

*adr1-L1* background. The *snc1*-enhancing phenotypes in *snc1 adr1-L1* are largely suppressed by *adr1* and fully suppressed by *adr1 adr1-L2* as observed in morphology, FW and the expression of *PR1* and *PR2* (Fig. 6a–c), suggesting that ADR1 and ADR1-L2 are indeed responsible for the enhanced immunity in *adr1-L1*.

We also quantified *ADR1* and *ADR1-L2* transcript levels in various *snc1 adr* mutant combinations by qPCR (Fig. 6d). *ADR1* transcript level is elevated in *snc1 adr1-L1* but not in *snc1 adr1-L2* when compared to *snc1* (Fig. 6d). Similarly, *ADR1-L2* transcript level is elevated in *snc1 adr1-L1* but not in *snc1 adr1* when compared to *snc1* (Fig. 6d). These results suggest that the overcompensation effect seems to be specific to *adr1-L1*, but not with *adr1* or *adr1-L2*.

### Loss of all three ADR members completely suppresses the phenotypes of the typical TNL autoimmune mutants *snc1* and *chs2-1*

When the *snc1 adr1 triple* (*adr1-1 adr1-L1-2 adr1-L2-4*) quadruple mutant was generated, a complete *snc1*-suppressing phenotype was observed (Fig. 6a under UBC and 7a under UNC growth conditions). This confirms that the enhanced autoimmune phenotype observed in *snc1 adr1-L1* requires the other two *ADR1* family members. In addition, all three members of the ADR1 family seem to be fully required for *snc1* signaling.

We then tested whether the autoimmune phenotypes caused by additional NLR gain-of-function mutants also require the combined action of the ADR1 helpers. We crossed the *adr1 triple* mutant into *chs2-1*, *chs3-1*, *slh1-9* and *uni-1D*, each of which exhibits autoimmune phenotypes under particular growth conditions (Table S1). The *uni-1D* mutant carries a missense mutation in a CNL (*At1g61180*) gene in Ws-0 (Wassilewskija), causing severe dwarfism and seedling lethality under certain conditions (Igari *et al.*, 2008). *uni-1D* was introgressed to Col-0 and *uni-1D*/+ plants were used for our cross with the *adr1 triple* mutant. The *Arabidopsis slh1* (*sensitive to low humidity 1*) mutant has a mutation in the WRKY domain of the atypical TNL RRS1 that causes activation of defense responses and hypersensitive cell death (Noutoshi *et al.*, 2005).

As shown in Fig. 7(b), the *adr1 triple* mutant completely suppressed *chs2-1* under *chs2-1*-phenotype-inducing growth conditions, although leaves from the suppressed, WT-sized plants were often curled. We observed weak or partial suppression of the autoimmune phenotypes of *chs3-1* encoding an atypical TNL with TNL-LIM fusion (Yang *et al.*, 2010), *uni-1D* (Igari *et al.*, 2008) and *slh1-9* (Noutoshi *et al.*, 2005), in each of the respective phenotype-inducing growth conditions (Figs 7c–e, S4). We also observed weak suppression of the seedling lethal phenotype for *uni-1D adr1 triple* plants under our short day conditions on plates and on soil (Fig. S4). Together, these results are consistent with a general helper function for the ADR1 family for NLR signaling (Bonardi *et al.*, 2011). More specifically, the ADRs seem to be fully required for typical TNL signaling. We collated all known epistasis data to address what possible common signaling pathway might function downstream of the ADR helper NLRs and found that loss of SA biosynthesis was the only function that also suppressed all of the tested gain-of-function NLR mutations (Table S1). This is consistent with the loss of pathogen-induced SA accumulation in the *adr1 triple* mutant (Bonardi *et al.*, 2011).

## Discussion

Here we report immunity-enhancing phenotypes of the loss-of-function helper nucleotide-building leucine-rich repeat (NLR) mutant *adr1-L1* in combination with *snc1*. Interestingly, the ADR1-L1 paralogs ADR1 and ADR1-L2 are required for this phenotype. Transcripts of *ADR1* and *ADR1-L2* are upregulated in *adr1-L1* mutant. Thus, it is plausible that transcriptional upregulation of *ADR1* and *ADR1-L2* may overcompensate for the loss of *ADR1-L1*, leading to the defense-enhancing phenotypes observed in *snc1*. Additionally, we provide genetic evidence that the ADR1 helper NLR family seems to be generally required for typical TNL-mediated immunity. This study extends our knowledge on the functional interplay among helper NLRs.

ADR1-L1 serves as a positive regulator of immunity redundantly with ADR1 and ADR1-L2 (Bonardi *et al.*, 2011). Using *snc1*-suppressing phenotype as a criterion, these three *ADR* genes seem to exhibit unequal redundancy, with *ADR1* apparently the leading and *ADR1-L1* the least contributor (Fig. 6). The unexpected *snc1*-enhancing phenotypes of *adr1-L1* loss-of-function alleles reveal an apparent negative role in plant defense. We sought to define the mechanism for this unexpected autoimmunity-enhancing effect. We first examined the possibility that ADR1-L1 regulates SNC1 turnover, as do several *muse* mutants identified in the same screen that exhibit enhanced autoimmune phenotypes due to increased SNC1 protein levels (Huang *et al.*, 2014a,b). Although heightened SNC1 levels were observed in *snc1 adr1-L1* double mutant plants compared to *snc1* (Fig. 3a), steady-state SNC1 protein accumulation was unaffected in *adr1-L1* or when the feedback transcriptional upregulation of *SNC1* was blocked by *pad4-1* (Fig. 3c,e). Therefore, ADR1-L1 does not seem to be involved in the stability of steady-state SNC1 protein.

Second, we tested the specificity of the autoimmunity-enhancing effect of *adr1-L1*. Although *adr1-L1* did not enhance the autoimmunity of *snc2-1D*, *snc4-1D*, *chs1-2*, *chs2-1* or *chs3-1* (Fig. S3), it did exhibit enhanced autoimmunity in *bal* and other *SNC1/snc1*-overexpression contexts, and in *lsd1-2* (Figs 5, S5). These observations suggest that the enhancement of the autoimmune phenotypes in *snc1* by *adr1-L1* is unlikely through a direct regulation of SNC1-mediated immunity.

How does the specificity of ADR1-L1 come about? One possibility is that the autoimmune-enhancing effects from *adr1-L1* rely on a certain threshold level of immune signaling (Fig. 8) defined by immune outputs such as the expression of defense-related genes. On the one hand, when the autoimmune phenotypes are weak, the level of enhancement from *adr1-L1* is not enough to be transformed into a significant plant size difference. On the other, when the background autoimmunity is too strong, it is more difficult to detect a marginal decrease in plant size due to increased immunity caused by the loss of ADR1-L1.

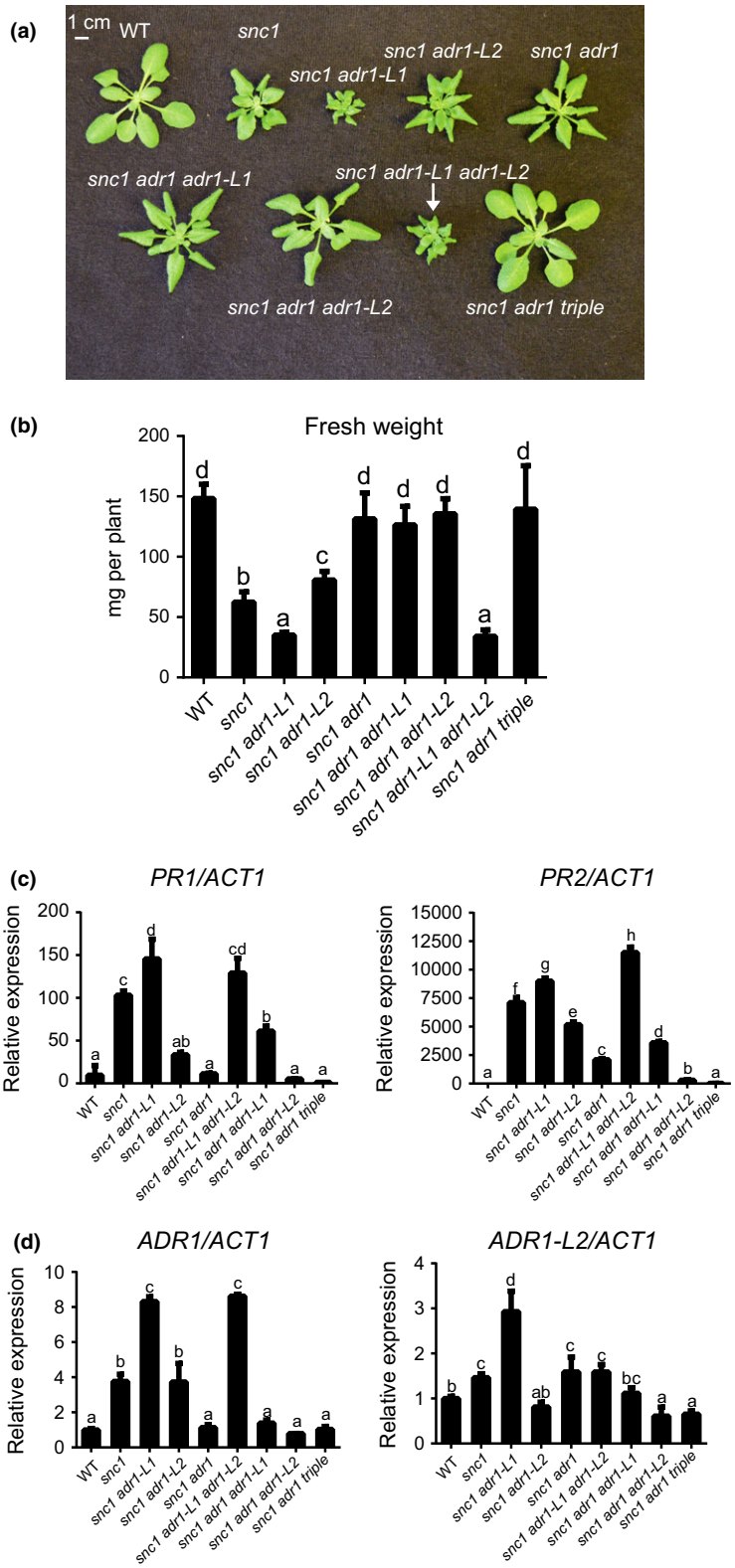


**Fig. 6** Characterization of combinatory *Arabidopsis* mutants between *snc1* and *adr*s. (a) Morphological phenotypes of 4-wk-old WT, *snc1*, *snc1 adr1-L1*, *snc1 adr1-L2*, *snc1 adr1*, *snc1 adr1-L1 adr1-L2*, *snc1 adr1 adr1-L1*, *snc1 adr1 adr1-L2* and *snc1 adr1 triple* plants grown at 22°C under long day conditions. (b) Fresh weights of 4-wk-old plants of the indicated genotypes grown at 22°C under long day conditions. One-way ANOVA was used to calculate the statistical significance between genotypes, as indicated by different letters ($P < 0.05$). Bars represent mean ± SD ($n = 6$). (c, d) Relative transcript levels of *PR1* and *PR2* (c); *ADR1* and *ADR1-L2* (d) in the indicated genotypes as determined by qRT-PCR. Total RNA was extracted from 4-wk-old plants grown at 22°C under long day conditions. *ACT1* was used to normalize the transcript levels. One-way ANOVA was used to calculate the statistical significance between genotypes, as indicated by different letters ($P < 0.05$). Bars represent mean ± SD ($n = 3$).

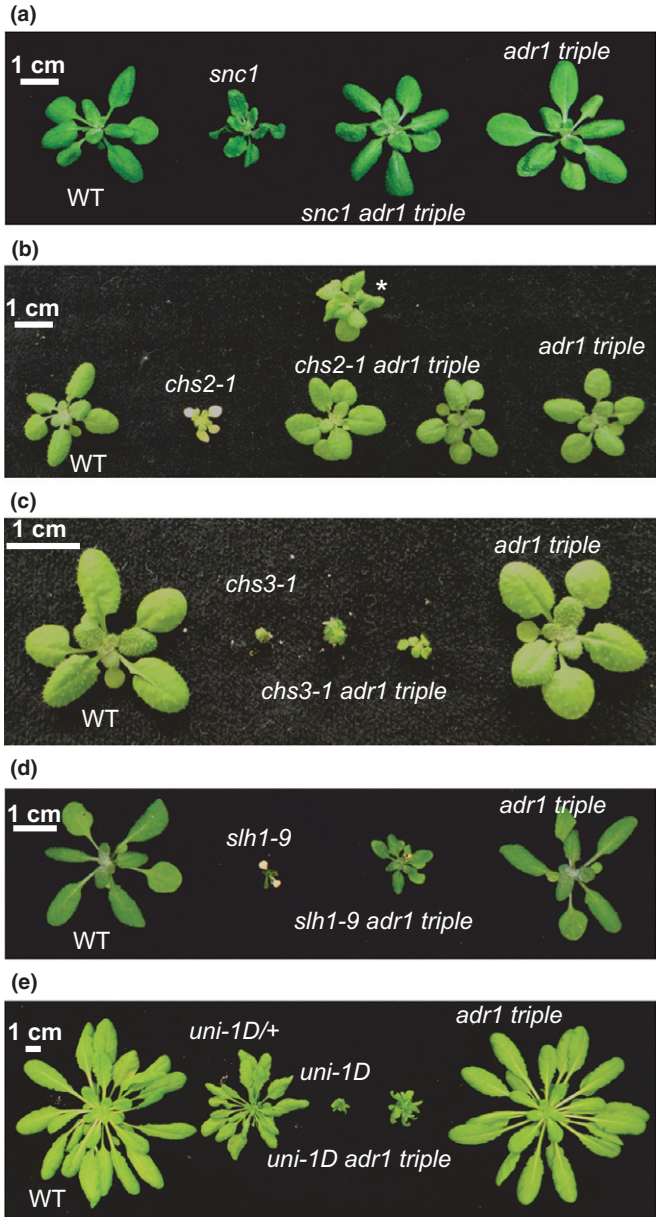


**Fig. 7** *Arabidopsis adr1 triple* mutant suppresses the autoimmune phenotypes of typical TNL gain-of-function mutants, but not others. (a) Morphological phenotypes of 4-wk-old WT, *snc1*, *snc1 adr1 triple* and *adr1 triple* mutant plants grown at 22°C under long day conditions. (b) Morphological phenotypes of 3-wk-old WT, *chs2-1*, *chs2-1 adr1 triple* and *adr1 triple* mutant plants grown at 16°C under long day conditions. Asterisk denotes the curled leaf suppression phenotype of some *chs2-1 adr1 triple* mutant plants. (c) Morphological phenotypes of 3-wk-old WT, *chs3-1*, *chs3-1 adr1 triple* and *adr1 triple* mutant plants grown at 16°C under long day conditions. (d) Morphological phenotypes of 3-wk-old WT, *slh1-9*, *slh1-9 adr1 triple* and *adr1 triple* mutant plants grown at 22°C under long day conditions. (e) Morphological phenotypes of 6-wk-old WT, *uni-1D/+*, *uni-1D, uni-1D adr1 triple* and *adr1 triple* mutant plants grown at 21°C/18°C under short day conditions (9 h : 15 h, light : dark).

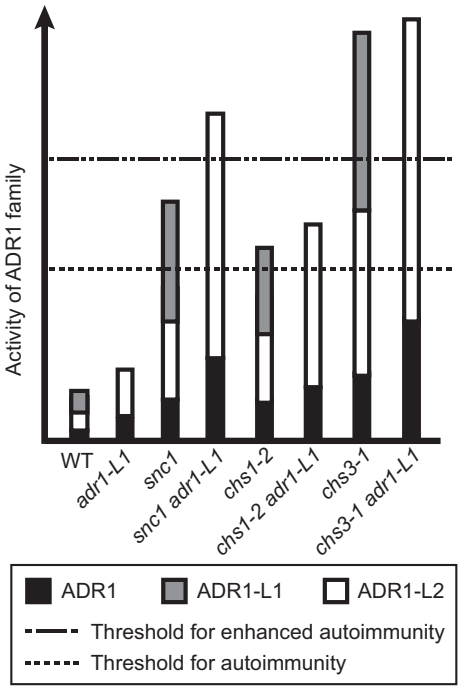


**Fig. 8** Working model: ADR1 and ADR1-L2 overcompensate for the loss of ADR1-L1 in defense regulation in *Arabidopsis*. Among the three *ADR* genes, *ADR1-L1* and *ADR1-L2* are expressed at higher levels, whereas *ADR1* is expressed at a lower level (Fig. S6; Roberts *et al.*, 2013). Therefore, there are potentially different amounts of the paralogous ADR proteins in WT plants required for their normal function. Loss of ADR1-L1 leads to heightened expression of *ADR1* and *ADR1-L2*, resulting in overcompensation of defense outputs. On the one hand, in WT, this overcompensation is not sufficient to lead to autoimmune response and enhanced disease resistance. However, in *snc1*, enhancement of the autoimmune phenotype becomes apparent. On the other, as in *chs1-2* where the autoimmunity is weak, the overcompensated ADR1 levels are insufficient to cross the autoimmune-enhancing threshold. By contrast, the autoimmunity as in *chs3-1* has reached a maximal limit and enhancement by *adr1-L1* is not observable at the level of plant size.

Gene expression may be upregulated to compensate for the loss of their functionally redundant paralogs (Diss *et al.*, 2014). The *Arabidopsis* R-SNARE (soluble *N*-ethylmaleimide sensitive factor attachment protein receptor) genes *VAMP721* and *VAMP722* are transcriptionally upregulated in the respective mutant to compensate for the loss of the other (Kwon *et al.*, 2008). In tomato, silencing of one ethylene receptor gene, *NR*, results in increased mRNA level of its redundant paralog *LeETR4* (Tieman *et al.*, 2000). Similar examples were also reported for redundant mammalian gene families, including retinoic acid receptor, retinoblastoma and connexin (Berard *et al.*, 1997; Mulligan *et al.*, 1998; Minkoff *et al.*, 1999). In a more recent example, Bethke *et al.* reported that *Arabidopsis* pectin methylesterases (PMEs) contribute to disease resistance against *Pseudomonas syringae*. Two PME loss-of-function mutants, *pme3* and *pme12,* exhibited enhanced disease resistance to *Pseudomonas syringae*, possibly by a similar overcompensation effect (Bethke *et al.*, 2014). Consistent with the paralogous gene overcompensation hypothesis, we repeatedly observed increased expression of *ADR1* and *ADR1-L2* in the *adr1-L1* mutant compared to WT (Figs 5a,b, S1). This increase is magnified in the *snc1* autoimmune mutant background (Fig. 5a,b). Similar to a previous report (Roberts *et al.*, 2013), we observed that individual *adr1*, *adr1-L1* and *adr1-L2* knock-out mutants affect *lsd1-2* phenotypes

differently under our growth conditions (Fig. S5), suggesting an unequal redundancy among the ADR1 family members. Further analyses of the microarray data from AtGenExpress (Schmid *et al.*, 2005; Winter *et al.*, 2007) revealed that the three *ADR1* gene family members are not expressed at the same level, nor do their expression levels respond to abiotic stresses to the same magnitude (Fig. S6). It is therefore possible that transcriptional upregulation of *ADR1* and *ADR1-L2* in the *adr1-L1* mutant would yield more ADR1 and ADR1-L2 proteins to replace ADR1-L1 in quantity, thus overcompensating for the loss of ADR1-L1 due to higher overall activity of the other two ADR1 family proteins (Fig. 8).

We cannot exclude the possibility that the proposed functional overcompensation could include a contribution from unequal protein stability or activity among the ADR1 family members. This situation, for example, occurs among two human retinoblastoma family members, p107 and p130. Loss-of-function p130 in T lymphocytes leads to higher levels of p107, and the predominant p130-E2F protein complex is replaced by a p107-E2F complex (Mulligan *et al.*, 1998). ADR1 and ADR1-L2 protein function or stability might be enhanced via the elimination of the less-effective family member ADR1-L1 as competitor.

How exactly loss of ADR1-L1 leads to upregulation of *ADR1* and *ADR1-L2* will be an interesting question to pursue in the future. It could be possible that the expression of the three *ADR* genes is coordinated by a common transcription factor that is able to sense the loss of ADR1-L1 and to enhance the expression of the other two paralogs. It is formally plausible that ADR1-L1 may be directly involved in transcriptional repression of its two paralogs. In both scenarios, loss of *ADR1-L1* would lead to an upregulation of *ADR1* and *ADR1-L2*, leading to enhanced immunity.

Besides the general role that ADRs play in regulating SA accumulation (Bonardi *et al.*, 2011), they also seem to have a more specific function in controlling TNL signaling. The complete *snc1*- or *chs2*-suppressing phenotypes by *adr1 triple* mutant (Figs 6, 7) resemble those of *pad4* and *eds1*, which are signaling intermediates of many typical TNLs upstream of SA synthesis (Wiermer *et al.*, 2005). These observations beg many questions to be addressed in the future. What is the relationship between EDS1/PAD4 and the ADRs? Where and how do these CNLs transduce signal downstream of TNLs? What protein partners are working together with these helper ADRs and how do the ADR protein dynamics change during defense? Answers to these questions will be vital to understand the involvement of these ADRs in the activation of sensor TNLs.

## Acknowledgements

We thank Dr Shuhua Yang (Chinese Agriculture University) for kindly sharing the *chs1-2*, *chs2-1* and *chs3-1* seeds, and Dr Yuelin Zhang (University of British Columbia) for seeds of *snc2-1D* and *snc4-1D*. We would like to acknowledge Ms Yuli Ding, Ms Yan Li and Dr Yuelin Zhang for Illumina sequencing and data analysis, and Mr David Kim for his assistance in mapping of *muse15-1*. This work was financially supported by a Discovery grant from Natural Sciences and Engineering Research Council of Canada (NSERC) and Dewar Cooper Memorial Fund from UBC to X.L. M.T. was partly supported by Chinese Scholarship Council, and O.X.D. was partly supported by a UBC Four-Year Fellowship. Work on this project at UNC was funded by the National Science Foundation (*Arabidopsis* 2010 Program Grant IOS-0929410 and IOS-1257373). V.B. was supported by the Human Frontier Science Program (LT00905/2006-L). F.E.K. was supported by the German Research Foundation (DFG; EL 734/1-1). J.L.D. is an Investigator of the Howard Hughes Medical Institute, supported by the HHMI and the Gordon and Betty Moore Foundation (GBMF3030).

## Author contributions

O.X.D., M.T., X.L., V.B. and J.L.D. designed the experiments. O.X.D. and M.T. performed most of the described experiments. V.W. characterized and mapped *muse15-2*. V.B., F.E.K. and L.K.W. generated the *lsd1-2 adr1-L1* mutant and combinatory mutants between autoimmune mutants and *adr1 triple*. O.X.D., J.L.D. and X.L. wrote the manuscript. All authors reviewed and edited the manuscript.

## References

**Berard J, Luo H, Chen H, Mukuna M, Bradley WE, Wu J. 1997.** Abnormal regulation of retinoic acid receptor beta2 expression and compromised allograft rejection in transgenic mice expressing antisense sequences to retinoic acid receptor beta1 and beta3. *Journal of Immunology* **159**: 2586–2598.

**Bethke G, Grundman RE, Sreekanta S, Truman W, Katagiri F, Glazebrook J. 2014.** Arabidopsis *PECTIN METHYLESTERASEs* contribute to immunity against *Pseudomonas syringae*. *Plant Physiology* **164**: 1093–1107.

**Bi D, Cheng YT, Li X, Zhang Y. 2010.** Activation of plant immune responses by a gain-of-function mutation in an atypical receptor-like kinase. *Plant Physiology* **153**: 1771–1779.

**Bonardi V, Tang S, Stallmann A, Roberts M, Cherkis K, Dangl JL. 2011.** Expanded functions for a family of plant intracellular immune receptors beyond specific recognition of pathogen effectors. *Proceedings of the National Academy of Sciences, USA* **108**: 16463–16468.

**Cheng YT, Li Y, Huang S, Huang Y, Dong X, Zhang Y, Li X. 2011.** Stability of plant immune-receptor resistance proteins is controlled by SKP1-CULLIN1-F-box (SCF)-mediated protein degradation. *Proceedings of the National Academy of Sciences, USA* **108**: 14694–14699.

**Chisholm ST, Coaker G, Day B, Staskawicz BJ. 2006.** Host–microbe interactions: shaping the evolution of the plant immune response. *Cell* **124**: 803–814.

**Collier SM, Hamel LP, Moffett P. 2011.** Cell death mediated by the N-terminal domains of a unique and highly conserved class of NB-LRR protein. *Molecular Plant–Microbe Interactions* **24**: 918–931.

**Dangl JL, Jones JD. 2001.** Plant pathogens and integrated defence responses to infection. *Nature* **411**: 826–833.

**Dietrich RA, Richberg MH, Schmidt R, Dean C, Dangl JL. 1997.** A novel zinc finger protein is encoded by the *Arabidopsis LSD1* gene and functions as a negative regulator of plant cell death. *Cell* **88**: 685–694.

**Diss G, Ascencio D, DeLuna A, Landry CR. 2014.** Molecular mechanisms of paralogous compensation and the robustness of cellular networks. *Journal of Experimental Zoology. Part B, Molecular and Developmental Evolution* **322**: 488–499.

**Frost D, Way H, Howles P, Luck J, Manners J, Hardham A, Finnegan J, Ellis J. 2004.** Tobacco transgenic for the flax rust resistance gene L expresses allele-

specific activation of defense responses. *Molecular Plant–Microbe Interactions* **17**: 224–232.

**Glazebrook J, Rogers EE, Ausubel FM. 1996.** Isolation of *Arabidopsis* mutants with enhanced disease susceptibility by direct screening. *Genetics* **143**: 973–982.

**Gou M, Shi Z, Zhu Y, Bao Z, Wang G, Hua J. 2012.** The F-box protein CPR1/CPR30 negatively regulates R protein SNC1 accumulation. *Plant Journal* **69**: 411–420.

**Grant JJ, Chini A, Basu D, Loake GJ. 2003.** Targeted activation tagging of the *Arabidopsis NBS-LRR* gene, *ADR1*, conveys resistance to virulent pathogens. *Molecular Plant–Microbe Interactions* **16**: 669–680.

**Huang S, Monaghan J, Zhong X, Lin L, Sun T, Dong OX, Li X. 2014a.** HSP90s are required for NLR immune receptor accumulation in *Arabidopsis*. *Plant Journal* **79**: 427–439.

**Huang X, Li J, Bao F, Zhang X, Yang S. 2010.** A gain-of-function mutation in the *Arabidopsis* disease resistance gene RPP4 confers sensitivity to low temperature. *Plant Physiology* **154**: 796–809.

**Huang Y, Chen X, Liu Y, Roth C, Copeland C, McFarlane HE, Huang S, Lipka V, Wiermer M, Li X. 2013.** Mitochondrial AtPAM16 is required for plant survival and the negative regulation of plant immunity. *Nature Communications* **4**: 2558.

**Huang Y, Minaker S, Roth C, Huang S, Hieter P, Lipka V, Wiermer M, Li X. 2014b.** An E4 ligase facilitates polyubiquitination of plant immune receptor resistance proteins in *Arabidopsis*. *Plant Cell* **26**: 485–496.

**Igari K, Endo S, Hibara K, Aida M, Sakakibara H, Kawasaki T, Tasaka M. 2008.** Constitutive activation of a CC-NB-LRR protein alters morphogenesis through the cytokinin pathway in *Arabidopsis*. *Plant Journal* **55**: 14–27.

**Jabs T, Dietrich RA, Dangl JL. 1996.** Initiation of runaway cell death in an *Arabidopsis* mutant by extracellular superoxide. *Science* **273**: 1853–1856.

**Jander G, Norris SR, Rounsley SD, Bush DF, Levin IM, Last RL. 2002.** *Arabidopsis* map-based cloning in the post-genome era. *Plant Physiology* **129**: 440–450.

**Johnson KC, Dong OX, Huang Y, Li X. 2012.** A rolling stone gathers no moss, but resistant plants must gather their MOSes. *Cold Spring Harbor Symposia on Quantitative Biology* **77**: 259–268.

**Jones JD, Dangl JL. 2006.** The plant immune system. *Nature* **444**: 323–329.

**Kwon C, Neu C, Pajonk S, Yun HS, Lipka U, Humphry M, Bau S, Straus M, Kwaaitaal M, Rampelt H *et al.* 2008.** Co-option of a default secretory pathway for plant immune responses. *Nature* **451**: 835–840.

**Li X, Clarke JD, Zhang Y, Dong X. 2001.** Activation of an EDS1-mediated *R*-gene pathway in the *snc1* mutant leads to constitutive, NPR1-independent pathogen resistance. *Molecular Plant-Microbe Interactions* **14**: 1131–1139.

**Li X, Kapos P, Zhang Y. 2015.** NLRs in plants. *Current Opinion in Immunology* **32C**: 114–121.

**Li Y, Li S, Bi D, Cheng YT, Li X, Zhang Y. 2010.** SRFR1 negatively regulates plant NB-LRR resistance protein accumulation to prevent autoimmunity. *PLoS Pathogens* **6**: e1001111.

**Macho AP, Zipfel C. 2014.** Plant PRRs and the activation of innate immune signaling. *Molecular Cell* **54**: 263–272.

**Minkoff R, Bales ES, Kerr CA, Struss WE. 1999.** Antisense oligonucleotide blockade of connexin expression during embryonic bone formation: evidence of functional compensation within a multigene family. *Developmental Genetics* **24**: 43–56.

**Mulligan GJ, Wong J, Jacks T. 1998.** p130 is dispensable in peripheral T lymphocytes: evidence for functional compensation by p107 and pRB. *Molecular and Cellular Biology* **18**: 206–220.

**Nawrath C, Metraux JP. 1999.** Salicylic acid induction-deficient mutants of *Arabidopsis* express *PR-2* and *PR-5* and accumulate high levels of camalexin after pathogen inoculation. *Plant Cell* **11**: 1393–1404.

**Noutoshi Y, Ito T, Seki M, Nakashita H, Yoshida S, Marco Y, Shirasu K, Shinozaki K. 2005.** A single amino acid insertion in the WRKY domain of the *Arabidopsis* TIR-NBS-LRR-WRKY-type disease resistance protein SLH1 (sensitive to low humidity 1) causes activation of defense responses and hypersensitive cell death. *Plant Journal* **43**: 873–888.

**Peart JR, Mestre P, Lu R, Malcuit I, Baulcombe DC. 2005.** NRG1, a CC-NB-LRR protein, together with N, a TIR-NB-LRR protein, mediates resistance against tobacco mosaic virus. *Current Biology* **15**: 968–973.

**Roberts M, Tang S, Stallmann A, Dangl JL, Bonardi V. 2013.** Genetic requirements for signaling from an autoactive plant NB-LRR intracellular innate immune receptor. *PLoS Genetics* **9**: e1003465.

**Schmid M, Davison TS, Henz SR, Pape UJ, Demar M, Vingron M, Scholkopf B, Weigel D, Lohmann JU. 2005.** A gene expression map of *Arabidopsis thaliana* development. *Nature Genetics* **37**: 501–506.

**Stokes TL, Kunkel BN, Richards EJ. 2002.** Epigenetic variation in *Arabidopsis* disease resistance. *Genes & Development* **16**: 171–182.

**Tang X, Xie M, Kim YJ, Zhou J, Klessig DF, Martin GB. 1999.** Overexpression of Pto activates defense responses and confers broad resistance. *Plant Cell* **11**: 15–29.

**Tao Y, Yuan F, Leister RT, Ausubel FM, Katagiri F. 2000.** Mutational analysis of the *Arabidopsis* nucleotide binding site-leucine-rich repeat resistance gene *RPS2*. *Plant Cell* **12**: 2541–2554.

**Tieman DM, Taylor MG, Ciardi JA, Klee HJ. 2000.** The tomato ethylene receptors NR and LeETR4 are negative regulators of ethylene response and exhibit functional compensation within a multigene family. *Proceedings of the National Academy of Sciences, USA* **97**: 5663–5668.

**Wang Y, Zhang Y, Wang Z, Zhang X, Yang S. 2013.** A missense mutation in CHS1, a TIR-NB protein, induces chilling sensitivity in *Arabidopsis*. *Plant Journal* **75**: 553–565.

**Wiermer M, Feys BJ, Parker JE. 2005.** Plant immunity: the EDS1 regulatory node. *Current Opinion in Plant Biology* **8**: 383–389.

**Winter D, Vinegar B, Nahal H, Ammar R, Wilson GV, Provart NJ. 2007.** An "Electronic Fluorescent Pictograph" browser for exploring and analyzing large-scale biological data sets. *PLoS ONE* **2**: e718.

**Xu F, Cheng YT, Kapos P, Huang Y, Li X. 2014.** P-loop-dependent NLR SNC1 can oligomerize and activate immunity in the nucleus. *Molecular Plant* **7**: 1801–1804.

**Xu F, Huang Y, Li L, Gannon P, Linster E, Huber M, Kapos P, Bienvenut W, Polevoda B, Meinnel T *et al.* 2015.** Two N-terminal acetyltransferases antagonistically regulate the stability of a nod-like receptor in *Arabidopsis*. *Plant Cell* **27**: 1547–1562.

**Yang H, Shi Y, Liu J, Guo L, Zhang X, Yang S. 2010.** A mutant CHS3 protein with TIR-NB-LRR-LIM domains modulates growth, cell death and freezing tolerance in a temperature-dependent manner in *Arabidopsis*. *Plant Journal* **63**: 283–296.

**Yang Y, Zhang Y, Ding P, Johnson K, Li X, Zhang Y. 2012.** The ankyrin-repeat transmembrane protein BDA1 functions downstream of the receptor-like protein SNC2 to regulate plant immunity. *Plant Physiology* **159**: 1857–1865.

**Yi H, Richards EJ. 2009.** Gene duplication and hypermutation of the pathogen Resistance gene *SNC1* in the *Arabidopsis bal* variant. *Genetics* **183**: 1227–1234.

**Zhang Y, Goritschnig S, Dong X, Li X. 2003.** A gain-of-function mutation in a plant disease resistance gene leads to constitutive activation of downstream signal transduction pathways in *suppressor of npr1-1, constitutive 1*. *Plant Cell* **15**: 2636–2646.

**Zhang Y, Yang Y, Fang B, Gannon P, Ding P, Li X, Zhang Y. 2010.** *Arabidopsis* snc2-1D activates receptor-like protein-mediated immunity transduced through WRKY70. *Plant Cell* **22**: 3153–3163.

## Supporting Information

Additional supporting information may be found in the online version of this article.

**Fig. S1** Three additional biological repeats showing that transcript levels of *ADR1* and *ADR1-L2* are consistently upregulated in *adr1-L1*.

**Fig. S2** *adr1-L1* fully suppresses the cell death phenotype of *lsd1-2* and *chs3-1*, but not that of *chs1-2*.

**Fig. S3** *adr1-L1* does not enhance the autoimmune phenotypes of *snc2-1D*, *snc4-1D*, *chs1-2*, *chs2-1* or *chs3-1*.

**Fig. S4** Partial suppression of the *uni-1D* autoimmune phenotypes by *adr1 triple* mutant.

**Fig. S5** *adr1*, *adr1-L1* or *adr1-L2* affects *lsd1-2* phenotypes differently.

**Fig. S6** *ADR1*, *ADR1-L1* and *ADR1-L2* have different expression levels.

**Table S1** Summary of epistasis analysis for gain-of-function NLR mutants

Please note: Wiley Blackwell are not responsible for the content or functionality of any supporting information supplied by the authors. Any queries (other than missing material) should be directed to the *New Phytologist* Central Office.